



## Evaluation of photo-assisted electro-Fenton process for the treatment of a saline petrochemical wastewater

Marzyeh Moattar<sup>a</sup>, Marzyeh Lotfi<sup>a</sup>, Sahand Jorfi<sup>b,c,\*</sup>

<sup>a</sup>Amirkabir University of Technology-Mahshahr Campus, Mahshahr, Iran, emails: marzie.moatar@gmail.com (M. Moattar), marzyeh.lotfi@gmail.com (M. Lotfi)

<sup>b</sup>Environmental Technologies Research Center, Ahvaz Jundishapur University of Medical Sciences, Ahvaz, Iran, email: sahand369@yahoo.com

<sup>c</sup>Department of Environmental Health Engineering, School of Health, Ahvaz Jundishapur University of Medical Sciences, Ahvaz, Iran

Received 29 July 2018; Accepted 26 January 2019

### ABSTRACT

Photo-electro-Fenton oxidation of a saline petrochemical wastewater was investigated. Effect of operational parameters including pH, voltage, initial COD concentration, and reaction time were investigated using response surface methodology in a central composite design. A quadratic polynomial model was generated by performing the minimum number of tests and consuming the minimum amount of material to determine the effect of dependent variable on COD removal efficiency in the design space. The results showed that the maximum COD removal was determined to be 65.953%, which was acquired in operational conditions of pH 3, voltage 3 V cm<sup>-1</sup>, reaction time of 144.8 min, and influent COD of 849.5 mg L<sup>-1</sup>. Kinetics study showed that the pseudo-first-order was best fitted with experimental results ( $R^2 = 0.9958$ ).

*Keywords:* Petrochemical wastewater; Advanced oxidation technology; Photo-electro-Fenton; Response surface methodology

### 1. Introduction

The petrochemical wastewater contains toxic and recalcitrant compounds which are harmful to the environment and human [1]. Contamination of water resources by these toxic compounds has led to the investigation of more efficient technologies for treatment of such wastewaters [2].

Physical treatment methods are only capable of removing solids and emulsified oils due to their mechanical mechanisms [3]. Although biological methods are environmentally friendly and efficient, their applications are associated with some limitations such as sensitiveness to toxics, need for a large area, time intensive reactions, low biodegradability of organics, and selective nature [4].

Advanced oxidizing processes (AOPs) are applied in nearly ambient temperature condition, producing highly

reactive radicals such as hydroxyl (HO<sup>•</sup>) [5–7]. The hydroxyl radical (HO<sup>•</sup>) is very effective in removal of organic compounds because of the fact that they are electrophilic reagents [6,8]. These radicals opt to react with the nearest organic compounds, which are rich in electrons, very fast and non-selectively and oxidize them [9]. Among different AOPs, Fenton reagent is of great importance. The main advantages of this method are the non-toxicity of the reagents, owning no residuals, and simplicity [10]. The mechanisms of Fenton reaction are presented in Eqs. (1)–(4) [11]:



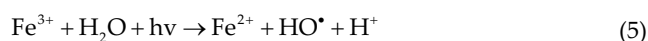
\* Corresponding author.

where 'RH' denotes organic pollutants,



As it is implied by Eq. (1), the ferrous ion acts as the catalyst and convert the hydrogen peroxide, which is a strong oxidizer, to the hydroxyl radical. The hydroxyl radical with an electronegativity of 2.8 eV has the second highest oxidizing potential after fluorine [12]. Based on Eq. (2), the hydroxyl radical oxidizes the organic compounds, which are rich in electrons. The electrochemical advanced oxidizing processes (EAOPs) act based on the Fenton reaction and are considered as the environmentally friendly processes. This method has gained lots of interest for treating wastewater [13]. One of the popular and considerable methods of EAOPs is electro-Fenton process. In this process, using a cathode, a sacrificing anode, and also an electricity source, an electro-chemical cell is developed, which acts based on the Fenton reaction. Electricity is a clean source of energy, which is utilized in this process. Thus, the process does not produce secondary pollutants [14]. As the electro-Fenton process does not produce any harmful reagent, it has been considered as an environmentally friendly method to treat wastewater.

In case of performing the E-Fenton reaction in a dark place, the reaction ceased after conversion of  $Fe^{2+}$  to  $Fe^{3+}$ . Utilization of ultraviolet favorably affects the rate of pollutants decomposition and leads to more efficient removal of pollutants. The ultraviolet leads to the formation of hydroxyl radical ( $HO^{\bullet}$ ) through the reductive reaction of  $Fe^{2+}$  to  $Fe^{3+}$  conversion Eq. (5). In addition, the ultraviolet directly converts the hydrogen peroxide to hydroxyl radical (Eq. (6)) [15–17]:



The current study focused on application of photo-electro-Fenton process for treatment of a real saline petrochemical wastewater as a first report dealing with real samples with the above-mentioned method. The influence of pH, initial COD concentration, reaction time, and applied voltage as input variable on the COD removal efficiency under UVA irradiation was studied through response surface methodology (RSM).

## 2. Materials and methods

### 2.1. Materials

Hydrochloric acid (37 wt%,  $MW = 36.5 \text{ g mol}^{-1}$ ) and sodium hydroxide ( $MW = 40 \text{ g mol}^{-1}$ ) were utilized to prepare acids and bases in different concentrations with distilled water to adjust the pH of the samples. All chemicals were of analytical grade and purchased from Merck, Germany. Iron and graphite electrodes with dimensions of

5 mm × 30 mm × 140 mm, respectively, as sacrificial anode and the cathode were purchased from a local area company.

### 2.2. Experimental set up and procedure

All experiments were performed in an electrochemical cell, including a 400 mL quartz chamber equipped with two iron and graphite electrode. They were located in 4 cm apart from each other. The electrodes were connected to a DC laboratory power supply with wire were purchased from local area company (MEGATEK, MP-3005, 30 V, 5 A, China). The voltage could be set using the tuning screw. Two UV-A lamps and two UV-C lamps (8 W) were set around the electrochemical cell. The electrochemical cell and the lamps were put in an MDF box (40 cm × 40 cm × 40 cm) to prevent exposure of the operators to the UV light (Fig. 1).

A magnetic stirrer (IKA-RH Basic 2) was utilized to completely mix; thus providing a uniform environment in the 400 mL reaction volume. The speed of the stirrer was set on 300 rpm and it was constant during all the experiments. A desired amount of sample was treated based on designed condition by the software in a distinct pH, initial COD concentration, voltage, and reaction time. COD removal efficiency was measured through determining the COD of the wastewater before and after treatment using a spectrophotometer (Hach, DR-5000, USA). The accuracy check of the apparatus was checked using KHP solution, which was prepared based on the standard method and its COD was equal to  $1,000 \text{ mg L}^{-1}$ . Due to effect of suspended solids on COD test, sample was put in the SETA centrifuge with speed of 3,000 rpm; for 10 min to remove suspended solids. The pH of the samples was adjusted using HCl 0.5 N and NaOH 0.5 N solutions and was monitored using pH meter Metrohm-827 (Germany). The wastewater samples used in this work were taken from a petrochemical plant located at Mahshahr city, Iran. Characteristics of the raw saline petrochemical wastewater are given in Table 1.

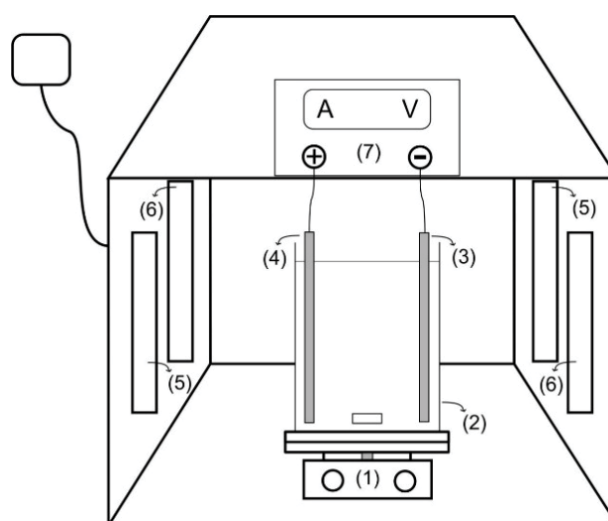


Fig. 1. Schematic diagram of photo-electro-Fenton batch reactor. (1) Electromagnetic mixer, (2) 400 mL quartz chamber, (3) iron anode, (4) graphite cathode, (5) UV-A lamp, (6) UV-C lamp, and (7) power supply.

Table 1  
Characteristics of raw wastewater

Parameter	Value	Average
COD (mg L <sup>-1</sup> )	500–1,000	750 ± 298
BOD <sub>5</sub> (mg L <sup>-1</sup> )	90–138	109 ± 65
BOD <sub>5</sub> /COD	0.18–0.138	0.125
TSS (mg L <sup>-1</sup> )	150–400	280 ± 27
TDS (mg L <sup>-1</sup> )	17,800–45,360	25,790 ± 4,300
EC	37,400–68,600	53,000 ± 10,900
pH	7.1–8.9	7.9 ± 0.7
Turbidity (NTU)	30–45	37 ± 5

### 2.3. Experimental design and modeling

RSM can be used in multiple systems in which effect of several independent variables on the response is investigated [18,19]. In addition, this method also can be used for optimization and finding the best level of variable for operational condition [20]. Central composite design (CCD) has been used widely in optimizing the photoelectro-Fenton process in literature, and was utilized in this study [21].

A four-factorial, three-level CCD consisting of 30 experimental runs was performed in the present work (Table 2), including six replications at the center point. The pH, voltage, initial COD concentration, and reaction time were considered as the independent variables while COD removal efficiency was considered as dependent variable (response; Eq. (7)). This study aimed to investigate the effect of the different ranges of the mentioned independent parameters on the response (COD removal efficiency):

$$\text{COD removal efficiency} = \frac{\text{COD}_e - \text{COD}_i}{\text{COD}_i} \times 100 \quad (7)$$

where COD<sub>e</sub> and COD<sub>i</sub> stand for final and initial COD, respectively. The values of the independent variables and their variation limits were determined considering the corresponding scientific literature, their results and the fact that reaching the highest possible efficiency with the minimum energy consumption.

Trail version of Design-Expert v.10.0.3 was utilized to analyze the curve fitting of the quadratic polynomial. RSM models are generally a full quadratic equation or the diminished form of this equation. The second-order model can be written as follows:

Table 2  
Experimental ranges and levels of independent process variables

Variable	Unit	Level		
		Low (-1)	Center (0)	High (+1)
COD <sub>i</sub>	mg L <sup>-1</sup>	500	750	1,000
pH	–	3	5	7
Voltage	V cm <sup>-1</sup>	3	4	5
Time	min	30	135	240

$$Y = \beta_0 + \sum_{i=1}^n \beta_i x_i + \sum_{i=1}^n \beta_{ii} x_i^2 + \sum_{i \neq j=1}^n \beta_{ij} x_i x_j + \varepsilon \quad (8)$$

where  $\beta_0$  is the value of the fixed response at the center point of the design,  $\beta_i$ ,  $\beta_{ii}$  and  $\beta_{ij}$  are the linear, quadratic, and interaction effect regression terms, respectively;  $x$  denotes the level of the independent variable;  $n$  is the number of independent variables; and  $\varepsilon$  is random error, while a second-order polynomial equation was derived as Eq. (9) [22]:

$$Y = \beta_0 + \beta_1 x_1 + \beta_2 x_2 + \beta_3 x_3 + \beta_{12} x_1 x_2 + \beta_{13} x_1 x_3 + \beta_{23} x_2 x_3 + \beta_{11} x_1^2 + \beta_{22} x_2^2 + \beta_{33} x_3^2 + \varepsilon \quad (9)$$

Analysis of variance (ANOVA) including lack of fit and F-test was performed to assess the accuracy and significance of the fitted model. In addition, the quality of the fitted polynomial model will be investigated using  $R^2$ , adjusted  $R^2$ , and predicted  $R^2$ . Close values of the mentioned parameters to unity indicated higher accuracy of the model [23].

## 3. Results and discussion

### 3.1. CCD modeling and statistical analysis

The values of the COD<sub>e</sub> for each experimental run are presented in Table 3. As it is shown, the COD removal efficiency spans between 41.2% and 71.1%, when no criteria was applied for optimization. The RSM model predicted a correlation, which is a second-order polynomial. The relation between the independent and dependent (response) variables is depicted in Eq. (10):

$$\begin{aligned} \text{Efficiency} = & +57.81 + 3.7 \times A + 5.38 \times B - 2.83 \times D + 0.24 \times AB - 1.32 \times \\ & AC + 0.66 \times AD + 0.56 \times BC - 1.15 \times BD - 0.26 \times CD - \\ & 5.52 \times A^2 - 3.10 \times B^2 + 3.11 \times C^2 + 4.25 \times D^2 \end{aligned} \quad (10)$$

Analyzing the accuracy of the developed model has a key role in validating the developed correlations [24]. Table 4 shows the ANOVA results for the developed model in prediction of the COD removal efficiency.

F-value is obtained through dividing the model mean square by residual mean square. Values of less than 0.05 for the prob > F indicate that the model is significant, whereas, the value greater than 0.1 usually imply that the model is insignificant. This value for the current study was determined to be less than 0.0001, which shows that the proposed model is significant. This means that the proposed model is correctly fitted and exhibits sufficient accuracy for modeling the aimed process. The parameter of “lack of fit” is “not significant”. This means that the data with high errors do not follow a logical trend.

The values of correlation coefficient  $R^2$ , adjusted  $R^2$ , and predicted  $R^2$  were determined to be 0.9599, 0.9225, and 0.8277, respectively. Closer values to the unity indicate higher accuracy of the proposed model. Thus, the developed method is accurate in predicting the response.

The value of the “adequate precision” indicates the signal dividing by noise [25]. Values greater than 4 are favorable for this parameter. In this study, this value was determined

Table 3  
Experimental design matrix and responses based on experimental runs proposed by CCD design

Run No	Independent variable				Response (removal efficiency)		
	X1	X2	X3	X4	Actual	Predicted	Residual
	COD <sub>i</sub>	Time	Voltage	pH			
1	1,000	135	4	5	48	45.83	2.17
2	500	30	3	7	54	54.08	-0.08
3	750	135	4	5	55.5	57.29	-1.79
4	1,000	30	3	3	67	66.49	0.51
5	1,000	240	5	3	53	54.26	-1.26
6	1,000	30	5	7	58	57.21	0.79
7	750	135	4	5	70	67.97	2.03
8	500	30	5	3	71.1	71.87	-0.77
9	1,000	30	5	3	41.2	41.67	-0.47
10	750	135	4	5	52	52.577	-0.577
11	500	30	3	3	49.2	48.537	0.663
12	1,000	240	3	3	60.4	60.38	0.02
13	1,000	240	3	7	50	49.05	0.95
14	500	135	4	5	55.2	54.65	0.55
15	750	135	3	5	57	58.16	-1.16
16	750	135	4	5	64	64.71	-0.71
17	1,000	240	5	7	47.5	48.593	-1.593
18	750	135	5	5	56.3	55.99	0.31
19	500	240	5	7	47.3	49.33	-2.03
20	750	135	4	5	61.33	60.08	1.25
21	750	135	4	7	57.33	57.73	-0.4
22	750	135	4	3	63.73	64.11	-0.38
23	1,000	30	3	7	63.33	64.88	-1.55
24	500	240	3	3	60	59.23	0.77
25	750	240	4	5	62	57.81	4.19
26	500	30	5	7	59.06	57.81	1.25
27	500	240	3	7	57.33	57.81	-0.48
28	750	30	4	5	55.5	57.81	-2.31
29	500	240	5	3	57.33	57.81	-0.48
30	750	135	4	5	58	57.81	0.19

to be 22.429, which shows acceptable signal for the response variable.

In accordance to the ANOVA results, the developed model is adequately capable to model the process and can be used to predict the COD removal efficiency in the design space.

### 3.2. Diagnostics and interaction between operational variables

#### 3.2.1. Normal plot of residual

It is possible to investigate the correlation of experimental and predicted values using the graph in which the normal probability is plotted vs. the internally studentized residuals [25]. In Fig. 2, there is a straight line which indicates that the residuals have a normal distribution.

#### 3.2.2. Effect of reaction time and initial COD concentration

In Fig. 3, the influence of initial COD (500–1,000 mg L<sup>-1</sup>) and time (30–240) variations on the COD removal efficiency

is shown. Figs. 3(a) and (b) show a two dimensional (2D) contour plot and a three-dimensional (3D) response surface of the model-predicted responses, respectively. The pH and voltage were kept constant on the center point values of 5 and 4 V cm<sup>-1</sup>, respectively, to investigate the effect of the other two parameters.

It was observed that along with initial COD up to 750 mg L<sup>-1</sup>, a raising trend of COD removal has been observed and no significant effect was appeared in higher concentrations and even some decrease in the COD removal was observed. On the other hand, as the time goes on, a progressive increase in the COD removal efficiency can be observed. According to these observations, the maximum COD removal efficiency was occurred at  $t = 230$  min and COD<sub>i</sub> = 849.

#### 3.2.3. Effect of voltage and initial COD

The applied current is a driving force to reduce the oxygen reduction, which results in generation of hydroxyl

Table 4  
ANOVA results of the quadratic polynomial model for photo-electro-Fenton treatment of raw petrochemical wastewater

Source	Sum of squares	Degree of freedom	Mean square	F-value	p-value	
Model	1,301.78	14	92.98	25.65	<0.0001	Significant
A	246.42	1	246.42	67.98	<0.0001	Significant
B	520.93	1	520.93	143.71	<0.0001	Significant
C	183.04	1	183.04	50.49	<0.0001	Significant
D	144.12	1	144.12	39.76	<0.0001	Significant
AB	0.90	1	0.90	0.25	0.6250	Not significant
AC	28.09	1	28.09	7.75	0.0139	Significant
AD	7.02	1	7.02	1.94	0.1843	Not significant
BC	5.06	1	5.06	1.40	0.2557	Not significant
BD	21.16	1	21.16	5.84	0.0289	Significant
CD	1.10	1	1.10	0.30	0.5894	Not significant
A <sup>2</sup>	78.93	1	78.93	21.78	0.0003	Significant
B <sup>2</sup>	24.95	1	24.95	6.88	0.0192	Significant
C <sup>2</sup>	25.12	1	25.12	6.93	0.0188	Significant
D <sup>2</sup>	46.73	1	46.73	12.89	0.0027	Significant
Residual	54.37	15	3.62			
Lack of Fit	30.35	10	3.04	0.63	0.7494	Not significant
Pure Error	24.02	5	4.80			

$R^2 = 0.9599$ ,  $R^2_{\text{Adjusted}} = 0.9225$ , adequate precision = 22.42, coefficient variation = 3.34(%), standard deviation = 1.90.  
A = CODi, B = pH, C = volt, D = time.

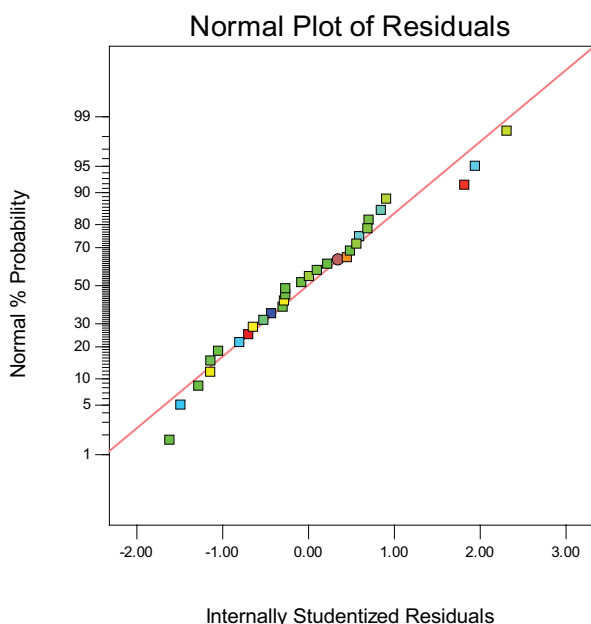


Fig. 2. Normal probability plot for COD removal efficiency (optimal conditions: pH = 3, voltage = 3 V cm<sup>-1</sup>, reaction time = 144.8 min, COD = 849.5 mg L<sup>-1</sup>).

radical in cathode. Greater applied current, which results from applying greater voltage on the system, increases the rate of hydrogen peroxide generation [26], thus, it will increase the hydroxyl generation in the medium [27]. The increase in the applied voltage and consequent generation

of ferrous ion, which is an electro-generation from ferric ion, (Eq. (11)) increases the efficiency of photo-electro-Fenton process through increasing the applied current.



Fig. 4 shows the influence of initial COD (500–1,000 mg L<sup>-1</sup>) and voltage (3–5 V cm<sup>-1</sup>) variation on the COD removal efficiency. The pH and reaction time were kept fixed on the center points of 5 and 135, respectively. Increasing the voltage led to an increase in the COD removal. Increasing the initial COD concentration up to 849 mg L<sup>-1</sup> enhanced the COD removal efficiency and higher values adversely affected the removal efficiency.

Considering the effects of voltage variation and initial COD concentration in the pre-determined ranges, it was concluded that the maximum value for the COD removal has occurred at COD<sub>i</sub> = 849 mg L<sup>-1</sup> and V = 5 v cm<sup>-1</sup>. Results are in accordance with literature [26].

### 3.2.4. Effect of pH and initial COD

The pH value has a key role in the photo-electro-Fenton process. Generally, Fenton process is performed in an acidic medium. The optimum pH value for the Fenton process is reported to be around 3 [28]. In the traditional Fenton process, the iron species starts to deposit as the ferric hydroxides in high pH values. On the other hand, the iron species develop stable complex with H<sub>2</sub>O<sub>2</sub> in low pH, which deactivates the catalysts [29]. As it is shown in Eq. (12), the acidic medium is a suitable condition for H<sub>2</sub>O<sub>2</sub> generation.

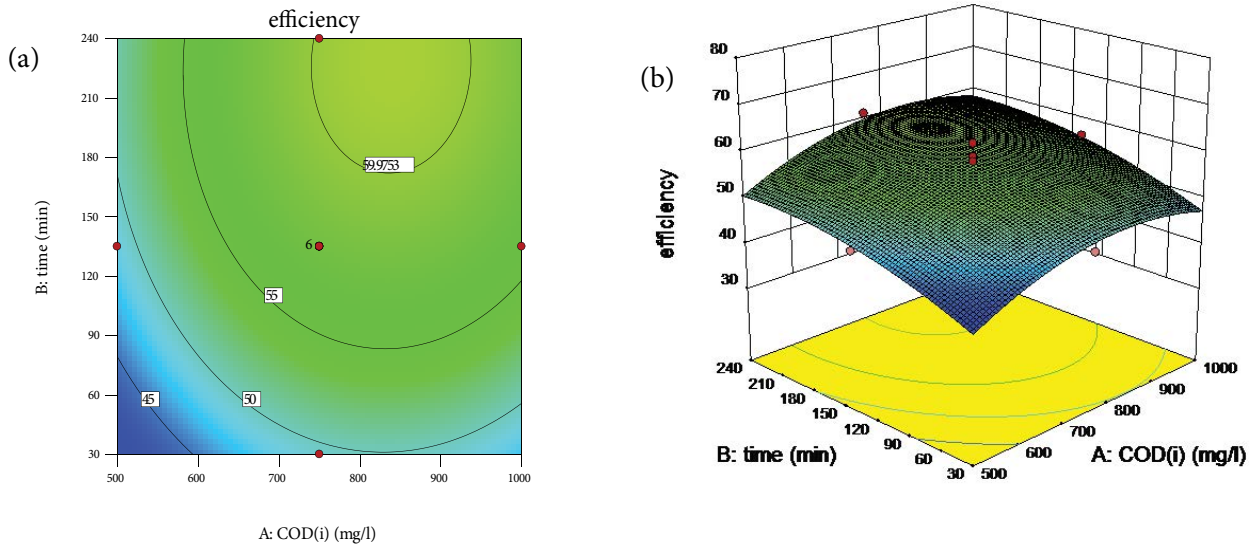


Fig. 3. Effect of initial COD concentration and reaction time on COD removal efficiency (a) 2D contour plots, (b) 3D response surface (optimal conditions: pH = 3, voltage = 3 V cm<sup>-1</sup>, reaction time = 144.8 min, COD = 849 mg L<sup>-1</sup>).

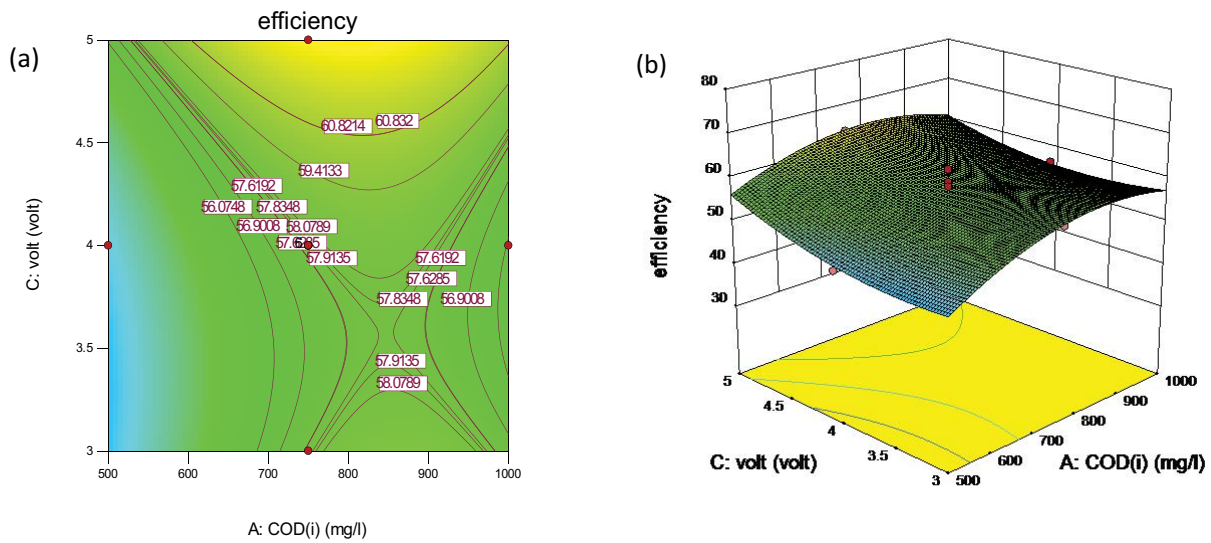


Fig. 4. Effect of initial COD and voltage on COD removal efficiency (a) 2D counter plots, (b) 3D response surface (optimal conditions: pH = 3, voltage = 3 V cm<sup>-1</sup>, reaction time = 144.8 min, COD = 849 mg L<sup>-1</sup>).



In pH values lower than 3, because of generation of some species such as oxinium ions (e.g., H<sub>3</sub>O<sub>2</sub><sup>+</sup>), the hydrogen peroxide will remain stable and no hydroxyl radical will be generated. In high pH values, the photo-electro-Fenton efficiency will quickly reduce, too. This is because of the fact that H<sub>2</sub>O<sub>2</sub> is unstable in basic solution. In neutral to basic pH values, the H<sub>2</sub>O<sub>2</sub> will be decomposed to oxygen and water with rate constants of 2.3 × 10<sup>-3</sup> min<sup>-1</sup> and 7.4 × 10<sup>-2</sup> min<sup>-1</sup>, respectively [30].

Fig. 5 shows the influence of initial COD concentration (500–1,000) and pH (3–7) variations on the COD removal

efficiency. COD removal efficiency increased in pH values around 3. According to Fig. 3, up to COD<sub>i</sub> = 849 mg L<sup>-1</sup>, the COD removal efficiency increased and after this point no significant improvement was observed. Considering the variations of the pH and initial COD in the investigated range, the maximum removal efficiency of 65% was achieved in COD<sub>i</sub> = 849 mg L<sup>-1</sup> and pH = 3.

### 3.3. Determination of intermediates

GC-MS analysis of real petrochemical wastewater before and after photo-electro-Fenton oxidation is shown in Figs. 6(a) and (b) to determine the main intermediate byproducts. According to Table 5, many complex organic compounds

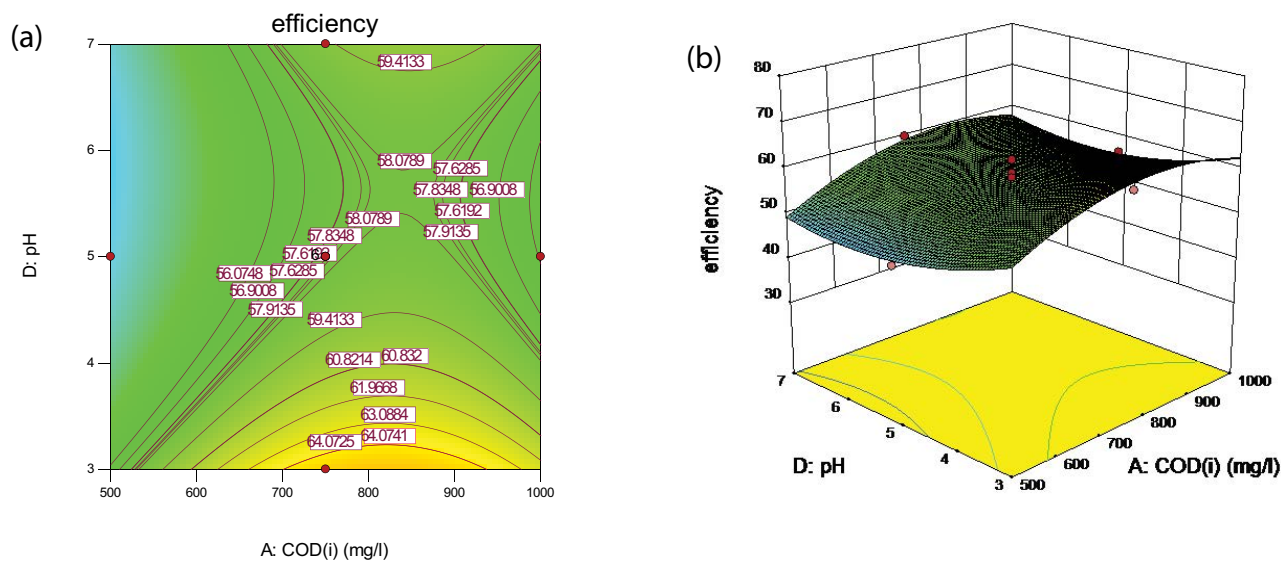


Fig. 5. Effect of initial COD and pH on COD removal efficiency (a) 2D contour plots, (b) 3D response surface (optimal conditions: pH = 3, voltage = 3 V cm<sup>-1</sup>, reaction time = 144.8 min, COD = 849 mg L<sup>-1</sup>).

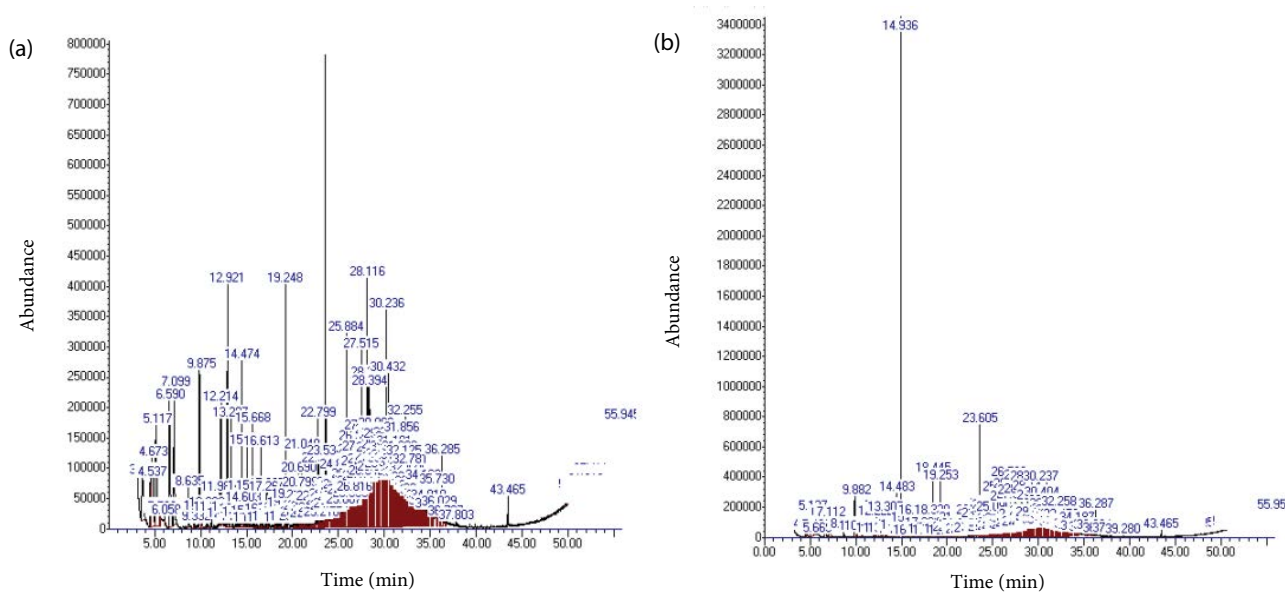


Fig. 6. GC-MS analysis of real petrochemical wastewater (a) before photo-electro-Fenton oxidation, (b) after photo-electro-Fenton oxidation.

available in the raw samples such as 13H-dibenzo[a,i] carbazole and tetradecamethyl were converted to simple and less harmful compound after treatment (Table 6). The majority of peaks observed in the GC-MS analysis corresponded to benzene and decane derivatives in different run times (Figs. 6(a) and (b)).

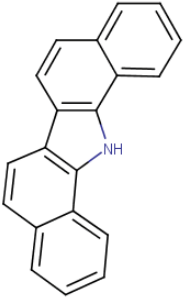
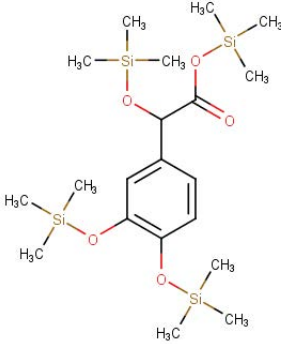
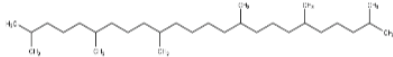
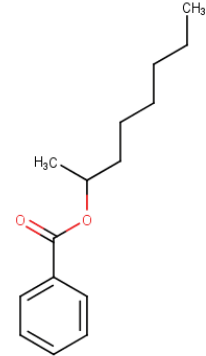
### 3.4. Optimization of photo-electro-Fenton oxidation

It is essential to determine the optimum values of all the independent parameters before utilizing a technology for application from laboratory to industrial scale. For this, the

desired objective for every independent variables as well as the response should be determined. As it is shown in Table 7, the favorable condition for this study was maximum COD removal efficiency, pH being in the predefined range, minimum voltage, maximum initial COD concentration, and minimum reaction time. Determining the condition in which the minimum energy and time are consumed is of great importance and optimization process.

Based on the desired objective for each parameter and its importance, the software generated some responses as they are listed in Table 8, of them are discussed here. Desirability of the responses is shown in the last column. Closer values to

Table 5  
Main compounds of petrochemical real wastewater

No	CAS#	Chemical formula	Structure	RT (min)	Substance
1	124-19-6	$C_9H_{18}O$		12.923	Nonanal
2	239-64-5	$C_{20}H_{13}N$		13.295	13H-Dibenzo[a,i]carbazole
3	37148-65-5	$C_{20}H_{40}O_5Si_4$		27.514	Benzeneacetic acid
4	111-01-3	$C_{30}H_{62}$		28.246	Squalene
5	6938-51-8	$C_{15}H_{22}O_2$		28.395	Octan-2-yl benzoate
6	40710-42-7	$C_{69}H_{138}O_2$		29.225	Nonahexacontanoic acid
7	40710-32-5	$C_{41}H_{84}O$		30.673	Hentetracontan-1-ol

the unity indicate that it is more likely to reach the predicted removal efficiency in the determined condition.

In the optimum condition of pH = 3,  $V = 3$  V,  $t = 144$  min, and  $COD_i = 849$  mg  $L^{-1}$ , the sample underwent treatment again to evaluate the response provided by the software.

Finally, the output COD was determined to be 310 mg  $L^{-1}$ . The efficiency was calculated to be 63.4% based on Eq. (1), which was in close agreement with the predicted efficiency by the software, which was 65.953%. ANOVA of the proposed model and also agreement of the software response with the

Table 6

Main intermediate byproducts of photo-electro-Fenton of petrochemical wastewater

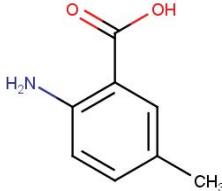
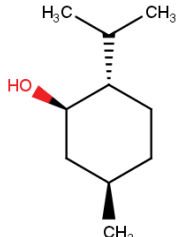
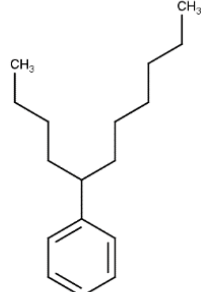
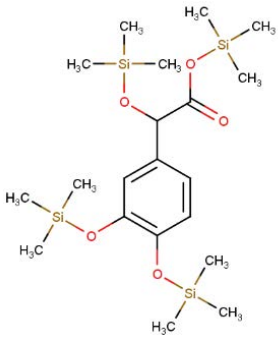
No	CAS#	Chemical formula	Structure	RT (min)	Substance
1	2941-78-8	$C_8H_9NO_2$		7.109	2-Amino-5-methylbenzoic acid
2	2216-51-5	$C_{10}H_{20}O$		14.937	L-menthol
3	629-50-5	$C_{13}H_{28}$		18.445	Tridecane
4	544-76-3	$C_{16}H_{34}$		25.889	Hexadecane
5	4537-15-9	$C_{17}H_{28}$		26.719	Benzene, (1-butylheptyl)
6	37148-65-5	$C_8H_8O_3$		27.514	Benzenacetic acid
7	629-78-7	$C_{17}H_{36}$		28.115	Heptadecane
8	593-45-3	$C_{18}H_{38}$		30.238	Octadecane

Table 7  
Conditions for the maximum COD removal efficiency for independent parameters consuming the minimum energy and time

Importance	Upper limit	Lower limit	Goal	Name
COD <sub>i</sub>	Maximize	500	1,000	+++
Time	Minimize	30	240	+++
Volt	Minimize	3	5	+++
pH	In range	3	7	+++
Efficiency	Maximize	41.2	71.1	+++++

Table 8  
Response for the maximum COD removal efficiency for the independent variables consuming the minimum energy and time

Number	COD <sub>i</sub>	Time	Volt	pH	Efficiency	Desirability
1	849.525	144.812	3	3	65.953	0.780
2	848.197	143.985	3	3	65.909	0.780
3	851.534	145.263	3	3	65.976	0.780
4	845.877	144.234	3	3	65.922	0.780
5	850.588	143.909	3	3	65.893	0.780

performed experiment indicate that the proposed model is capable of precisely predicting the removal efficiency in the design space.

In order to investigate the effect of light intensity on photo-electro-Fenton process in optimum conditions, two UV-C lamps was used. COD<sub>e</sub> = 275 mg L<sup>-1</sup> and COD removal efficiency = 67.6% was calculated. Results show that reducing the input light wavelength will increase the COD removal efficiency.

### 3.5. Kinetic study

Chemical kinetics represent the rate at which a reaction take place as well as the effective values on this rate. Rate of a reaction denotes the rate at which concentrations of the reactants and products change [31]. Decaying of the organic pollutants through the photo-electro-Fenton is represented in Eq. (2). As the HO• is highly active and cannot concentrate in the solution, its concentration will have a steady state through the treatment [32].

The rate of organic pollutants decomposition can be shown as follows:

$$\frac{d[RH]}{dt} = k[RH][OH^\bullet] \quad (13)$$

As the [HO•] value is fixed and will not change through the process, it is omitted from the kinetic equation and the COD concentration will be replaced as the representing factor of the organic pollutants [RH].

Several different kinetic models can be incorporated to evaluate the degree of a reaction [33]. However, the kinetic models of pseudo-first-order and pseudo-second-order are

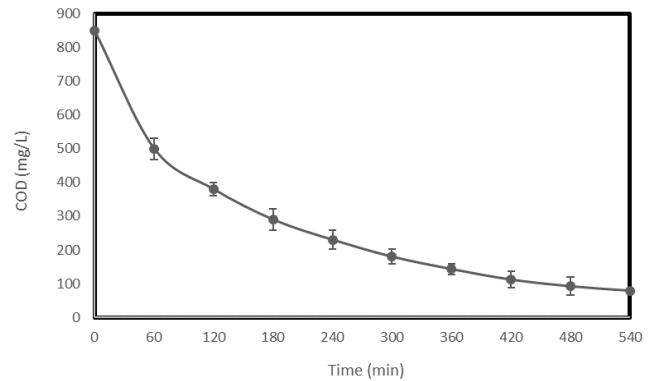


Fig. 7. Effect of reaction time on COD removal using photo-electro/Fenton process in optimum conditions (pH = 3, V = 3 V, COD(i) = 849 mg L<sup>-1</sup>).

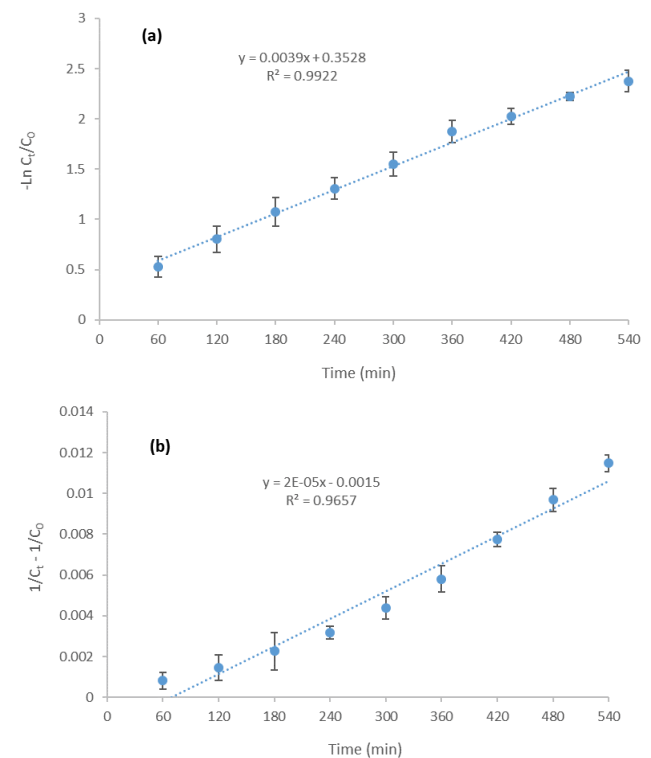


Fig. 8. Kinetics modeling of photo-electro-Fenton process in optimized conditions (pH = 3, V = 3 v, COD(i) = 849 mg L<sup>-1</sup>) for treatment of a saline petrochemical wastewater (a) pseudo-first-order model, (b) pseudo-second-order model.

more commonly used. Eqs. (14) and (15) show the kinetic equations models for the COD as the response [34].

$$\ln\left(\frac{COD_e}{COD_0}\right) = Kt \quad (14)$$

$$\frac{1}{COD_e} = \frac{1}{COD_0} + Kt \quad (15)$$

In order to determine the reaction kinetic in the optimum condition (pH = 3,  $V = 3$  V,  $\text{COD}_i = 849$  mg L<sup>-1</sup>), the treatment process was continued in the batch reactor and the COD was measured every 1 h. Fig. 7 showed the value of chemical oxygen demand of petrochemical real wastewater under photo-electro-Fenton system at optimum condition.

The modeling of the reaction kinetics based on pseudo-first-order and pseudo-second-order equations is depicted in Figs. 8(a) and (b).

The applicability of the kinetics models is determined using coefficient of determination  $R^2$ . Closer values to unity indicate better applicability of the proposed model for the desired data [35].

$R^2$  values for the three models of zero order, pseudo-first-order, and pseudo-second-order were 0.907, 0.9958, and 0.9659, respectively, thus the pseudo-first-order model exhibited the highest value.

#### 4. Conclusions

Results showed the effectiveness of photo-electro-Fenton process for COD removal from a saline petrochemical wastewater. A quadratic polynomial model was developed to assess the influence of four independent variables including pH, voltage, reaction time, and initial COD concentration on the response.  $R^2$  value of 0.9599 demonstrated sufficient accuracy to predict the response on the design space. All of the studied variables were significant. The optimum operational conditions were determined to be  $\text{COD}_i = 849$  mg L<sup>-1</sup>, pH = 3,  $V = 3$  V,  $t = 144$  min under UVA irradiation. Results of kinetic modeling proved that experimental data were best fitted with pseudo-first-order model. The influence of different types of anode and cathode, electrode distance could also be considered for future researches. Considering the saline and recalcitrant nature of studied petrochemical wastewater along with acceptable COD removal efficiency using photo-electro-Fenton process in optimized conditions in lab-scale level, it can be concluded that photo-electro-Fenton process is a reliable and efficient technology for treatment of such wastewaters and further studies are proposed in pilot-scale for obtaining sufficient data in term scaleup.

#### References

- [1] G. Barzegar, S. Jorfi, V. Zarezade, M. Khatebasreh, F. Mehdipour, F. Ghanbari, 4-Chlorophenol degradation using ultrasound/peroxymonosulfate/nanoscale zero valent iron: reusability, identification of degradation intermediates and potential application for real wastewater, *Chemosphere*, 201 (2018) 370–379.
- [2] E. Aranda, E. Marco-Urrea, G. Caminal, M.E. Arias, I. García-Romera, F. Guillén, Advanced oxidation of benzene, toluene, ethylbenzene and xylene isomers (BTEX) by *Trametes versicolor*, *J. Hazard. Mater.*, 181 (2010) 181–186.
- [3] A.L.N. Mota, A.F. Albuquerque, L.T.C. Beltrame, O. Chiavone-Filho, A. Machulek Jr., C.A.O. Nascimento, Advanced oxidation processes and their application in the petroleum industry: a review, *Brazil. J. Petrol. Gas.*, 2 (2008) 122–142;
- [4] S. Jorfi, S. Pourfadakari, B. Kakavandi, A new approach in sono-photocatalytic degradation of recalcitrant textile wastewater using MgO@Zeolite nanostructure under UVA irradiation, *Chem. Eng. J.*, 343 (2018) 95–107.
- [5] John C. Crittenden, R. Rhodes Trussell, David W. Hand, K.J.H.a.G. Tchobanoglous, *MWH's Water Treatment Principles and Design*, 3rd ed., John Wiley & Sons, Inc., Canada, 2012.
- [6] H. Choi, S.R. Al-Abed, D.D. Dionysiou, E. Stathatos, P. Lianos, TiO<sub>2</sub>-based Advanced Oxidation Nanotechnologies for Water Purification and Reuse, in: *Sustainability Science and Engineering*, Elsevier, Netherlands, 2010, pp. 229–254.
- [7] G. Boczkaj, A. Fernandes, Wastewater treatment by means of advanced oxidation processes at basic pH conditions: a review, *Chem. Eng. J.*, 320 (2017) 608–633.
- [8] M. Nurisepehr, S. Jorfi, R. Rezaei Kalantary, H. Akbari, R. Darvishi Cheshmeh Soltani, M. Samaei, Sequencing treatment of landfill leachate using ammonia stripping, Fenton oxidation and biological treatment, *Waste Manage. Res.*, 30 (2012) 883–887.
- [9] A.S. Stasinakis, Use of selected advanced oxidation processes (AOPs) for wastewater treatment – a mini review, *Global NEST J.*, 10 (2008) 376–385.
- [10] S. Wang, A Comparative study of Fenton and Fenton-like reaction kinetics in decolourisation of wastewater, *Dyes Pigm.*, 76 (2008) 714–720.
- [11] J. Ma, W. Song, C. Chen, W. Ma, J. Zhao, Y. Tang, Fenton degradation of organic compounds promoted by dyes under visible irradiation, *Environ. Sci. Technol.*, 395 (2005) 5810–5815.
- [12] M.B. Ray, J.P. Chen, L.K. Wang, S.O. Pehkonen, *Advanced Physicochemical Treatment Processes*, Humana Press, 2005.
- [13] E. Brillas, I. Sires, M.A. Oturan, Electro-Fenton process and related electrochemical technologies based on Fenton's reaction chemistry, *Chem. Rev.*, 109 (2009) 6570–6631.
- [14] C.-c. Jiang, J.-f. Zhang, Progress and prospect in electro-Fenton process for wastewater treatment, *J. Zhejiang Univ.-Sci. A*, 8 (2007) 1118–1125.
- [15] H. Chen, W. Liu, Z. Qin, ZnO/ZnFe<sub>2</sub>O<sub>4</sub> nanocomposite as a broad-spectrum photo-Fenton-like photocatalyst with near-infrared activity, *Catal. Sci. Technol.*, 7 (2017) 2236–2244.
- [16] F.C. Moreira, R.A.R. Boaventura, E. Brillas, V.J.P. Vilar, Electrochemical advanced oxidation processes: a review on their application to synthetic and real wastewaters, *Appl. Catal., B*, 202 (2017) 217–261.
- [17] P.V. Nidheesh, R. Gandhimathi, Trends in Electro-Fenton process for water and wastewater treatment: an overview, *Desalination*, 299 (2012) 1–15.
- [18] R.H. Myers, D.C. Montgomery, C.M. Anderson-cook, *Response Surface Methodology (process and product optimization using design experiments)*, 3rd ed., John Wiley & Sons, Inc., New Jersey, 2009.
- [19] A. Shojaie, M. Fattahi, S. Jorfi, B. Ghasemi, Hydrothermal synthesis of Fe-TiO<sub>2</sub>-Ag nano-sphere for photocatalytic degradation of 4-chlorophenol (4-CP): investigating the effect of hydrothermal temperature and time as well as calcination temperature, *J. Environ. Chem. Eng.*, 5 (2017) 4564–4572.
- [20] A. Khuri, S. Mukhopadhyay, *Response Surface Methodology*, John Wiley & Sons, Inc., London, Vol. 2, 2010, pp. 128–149.
- [21] P. Pakravan, A. Akhbari, H. Moradi, A. Hemati Azandaryani, A.M. Mansouri, M. Safari, Process modeling and evaluation of petroleum refinery wastewater treatment through response surface methodology and artificial neural network in a photocatalytic reactor using poly ethyleneimine (PEI)/titania (TiO<sub>2</sub>) multilayer film on quartz tube, *Appl. Petrochem. Res.*, 5 (2015) 47–59.
- [22] M.J.K. Bashir, S.S. Abu Amr, S.Q. Aziz, N.C. Aun, S. Sethupathi, Wastewater treatment processes optimization using response surface methodology (RSM) compared with conventional methods: review and comparative study, *Middle-East J. Sci. Res.*, 23 (2015) 244–252.
- [23] G. Barzegar, S. Jorfi, R.D.C. Soltani, M. Ahmadi, R. Saeedi, M. Abtahi, B. Ramavandi, Z. Baboli, Enhanced Sono-Fenton-like oxidation of PAH-contaminated soil using nano-sized magnetite as catalyst: optimization with response surface methodology, *Soil Sediment Contam.*, 26 (2017) 538–557.
- [24] B.K. Körbahti, Response surface optimization of electrochemical treatment of textile dye wastewater, *J. Hazard. Mater.*, 145 (2007) 277–286.
- [25] I. Arslan-Alaton, G. Tureli, T. Olmez-Hanci, Treatment of azo dye production wastewaters using Photo-Fenton like advanced

- oxidation processes: optimization by response surface methodology, *J. Photochem. Photobiol., A*, 202 (2009) 142–153.
- [26] S. Jorfi, S. Pourfadakari, M. Ahmadi, Electrokinetic treatment of high saline petrochemical wastewater: evaluation and scale-up, *J. Environ. Manage.*, 204 (2017) 221–229.
- [27] A. Singh, A. Verma, P. Bansal, J. Singla, Evaluation of the process parameters for electro Fenton and electro chlorination treatment of reactive black 5 (rb5) dye, *J. Electrochem. Soc.*, 164 (2017) 203–212.
- [28] M.M. Ghoneim, H.S. El-Desoky, N.M. Zidan, Electro-Fenton oxidation of sunset yellow FCF azo-dye in aqueous solutions, *Desalination*, 274 (2011) 22–30.
- [29] C.-T. Wang, W.-L. Chou, M.-H. Chung, Y.-M. Kuo, COD removal from real dyeing wastewater by electro-Fenton technology using an activated carbon fiber cathode, *Desalination*, 253 (2010) 129–134.
- [30] H. Shemer, K.G. Linden, Degradation and by-product formation of diazinon in water during UV and UV/H<sub>2</sub>O<sub>2</sub> treatment, *J. Hazard. Mater.*, 136 (2006) 553–559.
- [31] M. Ahmadi, S. Jorfi, R. Kujlu, S. Ghafari, R. Darvishi Cheshmeh Soltani, N. Jaafarzadeh Haghhighifard, A novel salt-tolerant bacterial consortium for biodegradation of saline and recalcitrant petrochemical wastewater, *J. Environ. Manage.*, 191 (2017) 198–208.
- [32] A.K. Abdessalem, N. Oturan, N. Bellakhal, M. Dachraoui, M.A. Oturan, Experimental design methodology applied to electro-Fenton treatment for degradation of herbicide chlortoluron, *Appl. Catal., B*, 78 (2008) 334–341.
- [33] F. Hayati, A. Isari, M. Fattahi, B. Anvaripour, S. Jorfi, Photocatalytic decontamination of phenol and petrochemical wastewater through ZnO/TiO<sub>2</sub> decorated on reduced graphene oxide nanocomposite: influential operating factors, mechanism, and electrical energy consumption, *RSC Adv.*, 8 (2018) 40035–40053.
- [34] N.P. Tantak, S. Chaudhari, Degradation of azo dyes by sequential Fenton's oxidation and aerobic biological treatment, *J. Hazard. Mater.*, 136 (2006) 698–705.
- [35] Y. Safa, H.N. Bhatti, Kinetic and thermodynamic modeling for the removal of Direct Red-31 and Direct Orange-26 dyes from aqueous solutions by rice husk, *Desalination*, 272 (2011) 313–322.